PHYSICAL REVIEW D **78,** 116001 (2008)

Shape of primary proton spectrum in multi-TeV region from data on vertical muon flux

A. V. Yushkov*
Sezione INFN di Napoli, I-80126, Napoli, via Cintia, Italy

A. A. Lagutin
Altai State University, 656049, Barnaul, Lenin prospect, Russia
(Received 3 June 2008; published 1 December 2008)

It is shown that the primary proton spectrum, reconstructed from sea-level and underground data on muon spectrum with the use of QGSJET 01, QGSJET II, NEXUS 3.97, and SIBYLL 2.1 interaction models, demonstrates not only model-dependent intensity, but also a model-dependent form. For correct reproduction of muon spectrum shape the primary proton flux should have a nonconstant power index for all considered models, except SIBYLL 2.1, with break at energies around 10–15 TeV and a value of exponent before break close to that obtained in the ATIC-2 experiment. To validate the presence of this break, understanding of inclusive spectra behavior in the fragmentation region in p-air collisions should be improved, but we show that is impossible to do on the basis of the existing experimental data on primary nuclei, atmospheric muon, and hadron fluxes.

DOI: 10.1103/PhysRevD.78.116001 PACS numbers: 95.85.Ry, 96.50.sb

I. INTRODUCTION

At present, information on the characteristics of hadronic interactions in fragmentation region is still scarce or missing and experiments with ''roman pots'' are anticipated to improve the situation. Some of this information, in principle, could be obtained with the use of the data on cosmic ray (CR) muon and hadron spectra, provided primary spectra are known with high precision, but that is not the case. The obvious obstacle here is that at high energies primary cosmic ray (PCR) fluxes, measured in direct experiments, themselves are functionals of various interaction parameters, plus their accuracy is appreciably affected by additional systematic effects [1–4]. In the series of our papers [5,6], we underlined that these effects can lead to underestimation of light nuclei fluxes and thus can explain discrepancy between measured and calculated muon fluxes for $E_\mu > 100$ GeV. Preliminary data of ATIC-2 [7], covering the gap between magnetic spectrometer and emulsion chamber experiments, seems to be in concordance with our conclusions, but the situation is more complicated in fact, as further consideration will show. The ATIC-2 slope of proton spectrum $\gamma_p = 2.63$ [8] for primary energies below 10 TeV is in remarkable contradiction with previously measured values $\gamma_p = 2.74$ and $\gamma_p = 2.80$ by RUNJOB [9] and JACEE [10] experiments correspondingly, but this discrepancy is removed by steepening in the ATIC-2 proton spectrum at energies above 10 TeV. These new data were already exploited in extensive calculations of muon and hadron fluxes with a number of interaction models at different atmospheric depths and zenith angles in [11], where it was shown that their use allows one to get reasonable agreement with most of the data under an appropriate choice of hadronic interaction parameters. In fact, it is not possible to obtain concordant conclusions on primary spectra or hadronic interaction parameters coming even from a much smaller subset of the experimental data. In this paper we demonstrate this on the basis of analysis of the data on muon flux at the vertical direction and only one set of the data on the hadron flux of EAS-TOP [12]. First, we use the data of sea-level and underground experiments to obtain conclusions on behavior of muon spectrum at sea level in the energy range 40 GeV–10 TeV. Further we analyze the influence of uncertainties in the muon data and interaction parameters on properties of reconstructed primary proton fluxes. Finally, we show that such a difference in approach and characteristics interaction models as SIBYLL 2.1 [13,14] and NEXUS 3.97 [15] can bring hardly distinguishable predictions on muon and hadron fluxes.

II. SEA-LEVEL MUON SPECTRUM FROM UNDERGROUND EXPERIMENTS DATA

The depth-intensity relation, needed for reconstruction of the sea-level muon spectrum, may be obtained via numerical solution of the one-dimensional transport equation. In an adjoint approach, this equation has the following form [16]:

$$\frac{\partial \bar{q}(t,E)}{\partial t} + \sigma \bar{q}(t,E) - \sum_\beta \int_{E_{\rm th}}^{E} dE' W_\beta(E,E') \bar{q}(t,E') = D(t,E).$$

Here $\bar{q}(t,E)$ is the survival probability of muon with energy E, being born at the distance t from the detector; σ is the total interaction cross section, $W_\beta(E,E')$; $\beta = i, r, p, h$ are the differential cross sections for processes of ionization,

*yushkov_av@mail.ru

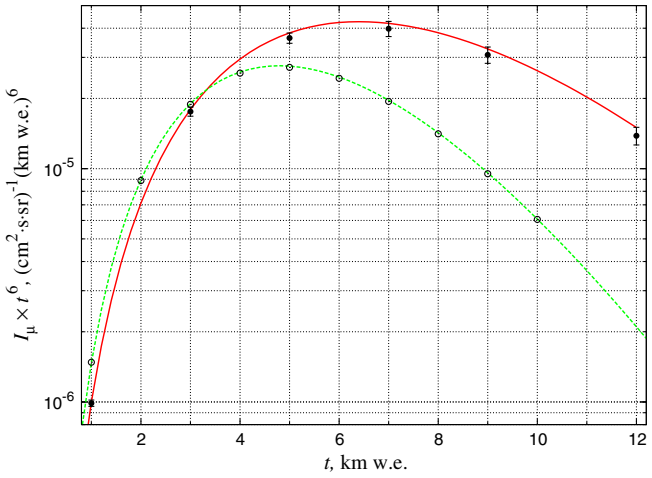

FIG. 1 (color online). Muon intensity in water and in standard rock. Water (muon spectrum at sea level from [18]): solid line—present work; closed circles—MUM [18], error bars show uncertainty due to ±1% variation of total muon energy losses. Standard rock (muon spectrum at sea level from [39]): dashed line—present work; open circles—MUSIC [40].

bremsstrahlung, pair production, and photonuclear interaction correspondingly; $D(t, E)$ is the detector sensitivity function. The numerical method, applied for solution of this equation [17], allows one to avoid any approximations (such as continuous losses one) and to obtain muon intensities at large depths of matter with account of fluctuations in all muon interaction processes. Accuracy of our calculations of muon survival probabilities and intensities was thoroughly examined in [17] and comparison with the results of Monte Carlo codes MUM [18] and MUSIC [19] is presented in Fig. 1. Anticipating further discussion of sea-level muon spectrum behavior, it is necessary to note that our calculations give an upper estimate of muon flux at large depths in comparison with MUM, because of the use of ~1% lower muon energy losses [17].

To describe the data on muon intensity underground and at sea level, and to estimate influence of uncertainty in muon flux data on reconstruction of primary proton flux, we used two parametrizations in the simple form, proposed in the work of Bogdanova *et al.* [20]. The original fit for the vertical from [20],

$$S_\mu(E) = 18/(E + 145)/(E + 2.7)^{2.7}, \ (\text{cm}^2\,\text{s}\,\text{sr}\,\text{GeV})^{-1}, \quad (1)$$

provides good agreement with the data at sea level (Fig. 2), but leads to underestimation of the muon flux for the depths below 6 km water equivalent (w.e.) (Fig. 3).

To match better underground data for the depths 2–6 km w.e. we shall also apply a modified fit with slightly <10% increased intensity in the multi-TeV region,

$$S_\mu(E) = 20.8/(E + 194.3)/E^{2.71}, \ (\text{cm}^2\,\text{s}\,\text{sr}\,\text{GeV})^{-1}. \quad (2)$$

As it is seen from Fig. 3, for depths from 4 km w.e. up to 8 km w.e., corresponding to ~2.5–10 TeV median muon energies at sea level, use of this spectrum provides good agreement with the data of LVD [21], BNO [22], and Frejus [23,24] collaborations and leads to underestimation of data of MACRO [25] and Soudan [26,27] experiments.

Our consideration will touch muon energies only above 40 GeV, to exclude different effects, not related to high-energy hadronic interactions features, such as geomagnetic effect, influence of uncertainties in low-energy interaction models, or even absorption of low-energy muons in ground as in the case of the L3 + C detector.

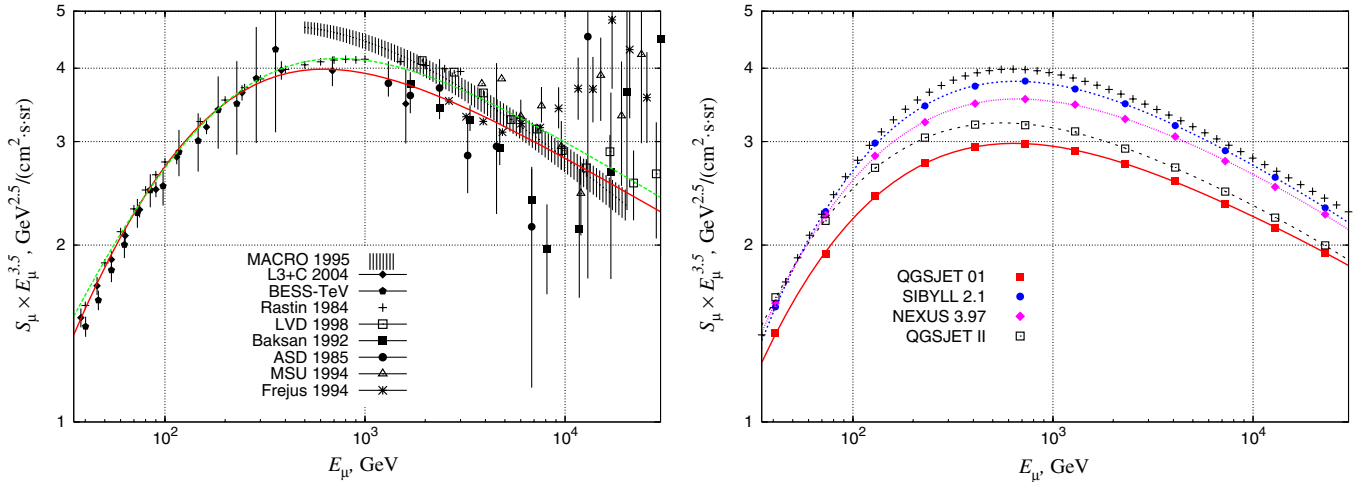

FIG. 2 (color online). Sea-level muon spectrum. Experimental data: [25] MACRO 1995, [41] L3 + C 2004, [42] BESS-TeV, [43] Rastin, [21] LVD 1998, [44] Baksan 1992, [45] ASD 1985, [46] MSU 1994, [23] Frejus 1994. Left: Solid line—muon spectrum (1); dashed line—muon spectrum (2). Right: Muon spectra at sea level for PCR spectra from [34] with high helium flux. Muon spectrum parametrization (1) is shown with crosses.

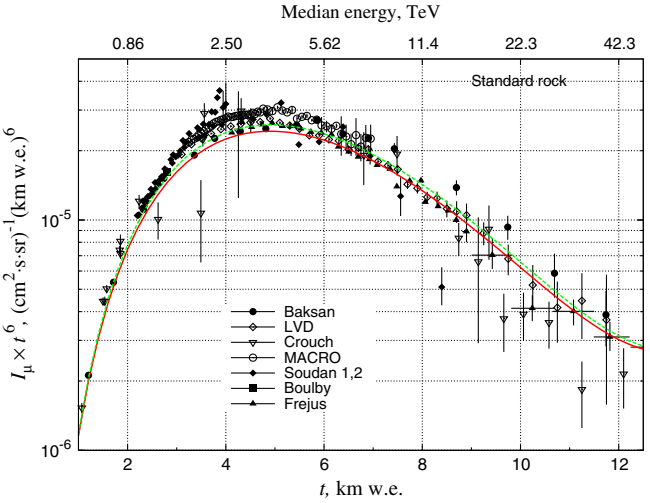

FIG. 3 (color online). Vertical muon intensity in standard rock. Experimental data: [22] Baksan, [21] LVD, [47] Crouch, [25] MACRO, [26,27] Soudan 1, 2, [48] Boulby, [23,24] Frejus. Present work calculations: solid line—for muon spectrum (1); dashed line—for muon spectrum (2). Neutrino induced muon contribution is taken from [49].

III. CALCULATIONS TECHNIQUE OF ATMOSPHERIC MUON AND HADRON FLUXES

Average numbers of hadrons $N_h(E_N, >E_{th})$ and muons $N_\mu(E_N, >E_{th})$ with energies above E_{th} in EAS from primary nucleon of energy E_N were obtained with the help of one-dimensional hybrid code CONEX [28,29] in the regime of cascade equations solution for interaction models QGSJET 01 [30], SIBYLL 2.1 [14], NEXUS 3.97 [15], and QGSJET-II-03 [31–33]. To get a differential spectrum of hadrons (or in the same way of muons) for some energy E_0, the following simple formula had been used:

$$S_h(E_0) = [I_h(>E_0 - \Delta E) - I_h(>E_0 + \Delta E)]/2\Delta E. \quad (3)$$

Here $I_h(>E_0)$ is the integral spectrum of hadrons

$$I_h(>E_0) = \int_{E_0}^{E_\infty} S_N(E_N) N_h(E_N, >E_0) dE_N$$

for primary nucleon spectrum $S_N(E_N)$.

The interval width ΔE must be chosen to provide the difference between integral intensities in (3) to be much larger than calculation error. Test computations for $\Delta E = 0.01E_0$, $0.02E_0$, $0.05E_0$ and observation levels 820 and 1030 g/cm^2 for energy $E_0 = 1$ TeV brought to differential flux values lying within 3% from each other. Change of upper integration limit E_∞ in formula for $I_h(>E_0)$ from $10^4 \times E_0$ to $10^5 \times E_0$ gives less than 1% increase of differential flux. Lastly, an increase of number of primary energy bins in $N_h(E_N, >E_0)$ from 10 to 20 per order introduces ~2% variation to differential flux value. The listed error sources partially compensate each other and the total error of our calculations does not exceed 3%. The calculations were performed for the set of energies, coinciding with the set from the EAS-TOP experiment paper [12].

IV. SEA-LEVEL MUON FLUXES

As a basic model of PCR nuclei spectra, the parametrizations from [34] were chosen. Nuclei with $A \geq 4$ were treated in the framework of the superposition model, high accuracy of this approach is well known and was checked by our calculations with the use of CONEX both for muons and hadrons once again.

A comparison of the calculated muon fluxes with the experimental data, presented in Fig. 2, reveals a familiar picture of high-energy muon deficit. The reasons of its appearance were considered in our previous papers [5,6] and they still hold true regardless of the fact that three more interaction models were included in our analysis. All interaction codes, except QGSJET 01, satisfactorily describe data on muon flux only up to $E_\mu \sim 100$ GeV and then one by one fail to do it. Accounting that such muon energies correspond to primary energies above 1 TeV, studied with balloon (satellite)-borne emulsion chambers, we related muon deficit to underestimation of primary light nuclei fluxes taking place in these experiments [5,6]. Unfortunately, disagreement between the models in the muon fluxes also appears at energies around 100 GeV, thus making impossible precise reconstruction of the primary nucleon spectrum for $E_{prim} > 1$ TeV. In fact, in such conditions there are no reasons to rule out any of the models, except QGSJET 01, which leads to remarkable disagreement with the experiment even in the range of reliable magnetic spectrometers data on PCR and muon spectra.

To find out why the models differ in the predicted muon fluxes, let us consider quite characteristic energy 1.29 TeV, where discrepancies between the models reach appreciable values and the data on muons from underground installations are yet quite reliable. Contributions of primary protons to the differential flux of muons of the given energy, presented in Fig. 4, show that spread in muon fluxes between the interaction models is entirely due to uncertainties in the description of $\pi^\pm$, $K^\pm$-spectra in fragmentation region $x = E_{\pi,K}/E_{prim} > 0.1$. Since inclusive muon flux is sensitive nearly only to the characteristics of the very first primary particle interaction, hence, the harder these spectra are in the particular model, the larger muon intensity its use leads to. For the lower values of x, i.e. for $E_{prim} > 10$ TeV, all the models give practically the same muon yields. As noted above, in view of the uncertain situation with primary spectra for $E_{prim} > 1$ TeV, one cannot give preference to any of the models in comparison with the others. If we were to demand the minimal disagreement with the direct measurements data on PCR spectra, then obviously SIBYLL 2.1 satisfies this requirement the best, or, on the other hand, one could say that it

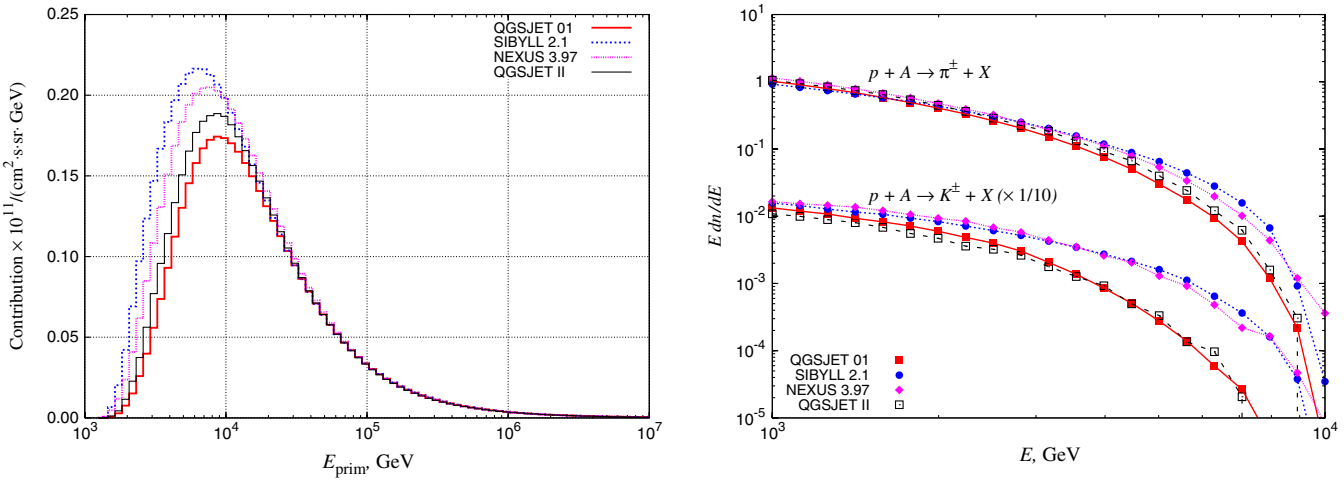

FIG. 4 (color online). Left: Contribution of primary protons with energies E_{prim} to the muon differential spectrum at sea level for $E_\mu = 1.29$ TeV. Right: Inclusive spectra $p + A \rightarrow \pi^\pm + X$ and $p + A \rightarrow K^\pm + X$ (scaled down by 10) for incident proton with energy 10 TeV.

provides the most acceptable description of $\pi^\pm$, $K^\pm$ production spectra in p-air collisions in fragmentation region. We shall discuss this affirmation in detail below.

V. PROTON SPECTRUM FROM MUON DATA

From the previous consideration, it is clear that reconstructed fluxes of protons shall be higher than measured in emulsion chamber experiments, but can be comparable with recently obtained data of the ATIC-2 group [7]. We performed the reconstruction simply by picking up appropriate primary proton flux parameters in order to minimize deviation of the obtained muon fluxes from the parametrizations (1) and (2).

First, let us consider an attempt to minimize maximal deviation from spectra (1) and (2) for $E_\mu =$ 40 GeV–10 TeV, in assumption that the primary proton spectrum can be described by the single power-law function $J_p = AE^{-\gamma_p}$ in the entire energy range 100 GeV–500 TeV. In Fig. 5 and in Table I, one can find the results of this reconstruction; upper and lower lines for each muon spectrum parametrization in Fig. 5 correspond to low and high helium flux fits [34]. As expected, the obtained spectra are flatter than measured by the RUNJOB and JACEE groups, but, except for the QGSJET 01 model, agree well with ATIC-2 results [7]. Figure 6 shows that in this case it is possible to achieve agreement with the fitted muon spectrum within 10%, but only SIBYLL 2.1 reproduces its shape correctly; with other models it is not possible to get right muon spectrum slope variation. We should also note that this behavior turned out to be insensitive to the choice of helium flux parametrization. As a result, there is a dip in the ratio of the muon flux, obtained from fitting of proton spectrum, to the parametrizations (1) and (2) for energies around 1 TeV, where the underground data were already underestimated (overestimation of muon flux at higher energies does not compensate this effect completely), and growth in the small energies range, which brings contradiction with low-energy $E_\mu < 40$ GeV data. Parametrization (2) was also projected to make muon spectrum slope variation less sharp, but this led to problems with its fitting in the ~100 GeV energy range, as seen from Fig. 6 (right panel) for SIBYLL 2.1 and NEXUS 3.97 models. The problem with muon spectrum shape matching is better illustrated by the upper left panel of Fig. 7, where it is shown that correct reproduction of muon spectrum for energies below 1 TeV with a single power-law proton spectrum leads to appreciable overestimation of muon flux at higher energies. There are three possible explanations or solutions of this problem. First, the discrepancy can be completely removed by choice of appropriate interaction parameters, e.g. similar to those in SIBYLL 2.1. Another argument which can be given is that the data on muon flux for energies above 1 TeV are not so definite to claim their inconsistency with the calculations, but it does not look well supported by underground data (see Fig. 3 and calculations [17,35]). The last possibility is to assume that the primary proton spectrum is not monotonous and either has a sharp break or a slowly changing exponent γ_p. Let us consider the latter assumption, which finds experimental [7] and theoretical [8,36,37] justifications, in more detail. The results for the simple case with break (Fig. 7), which allows one to achieve a correct description of muon spectrum shape with right asymptotic and deviation in flux value <3%, show that a small difference between spectra (1) and (2) results not only in different proton intensities, but also in break positions. The latter lies for parametrization (2) in the primary energy range 10–15 TeV, the change in power index reaches appreciable values up to $\Delta\gamma_p \approx 0.15$ for QGSJET 01 and QGSJET II models (Table I). Proton spectra, obtained from muon flux (2), with QGSJET

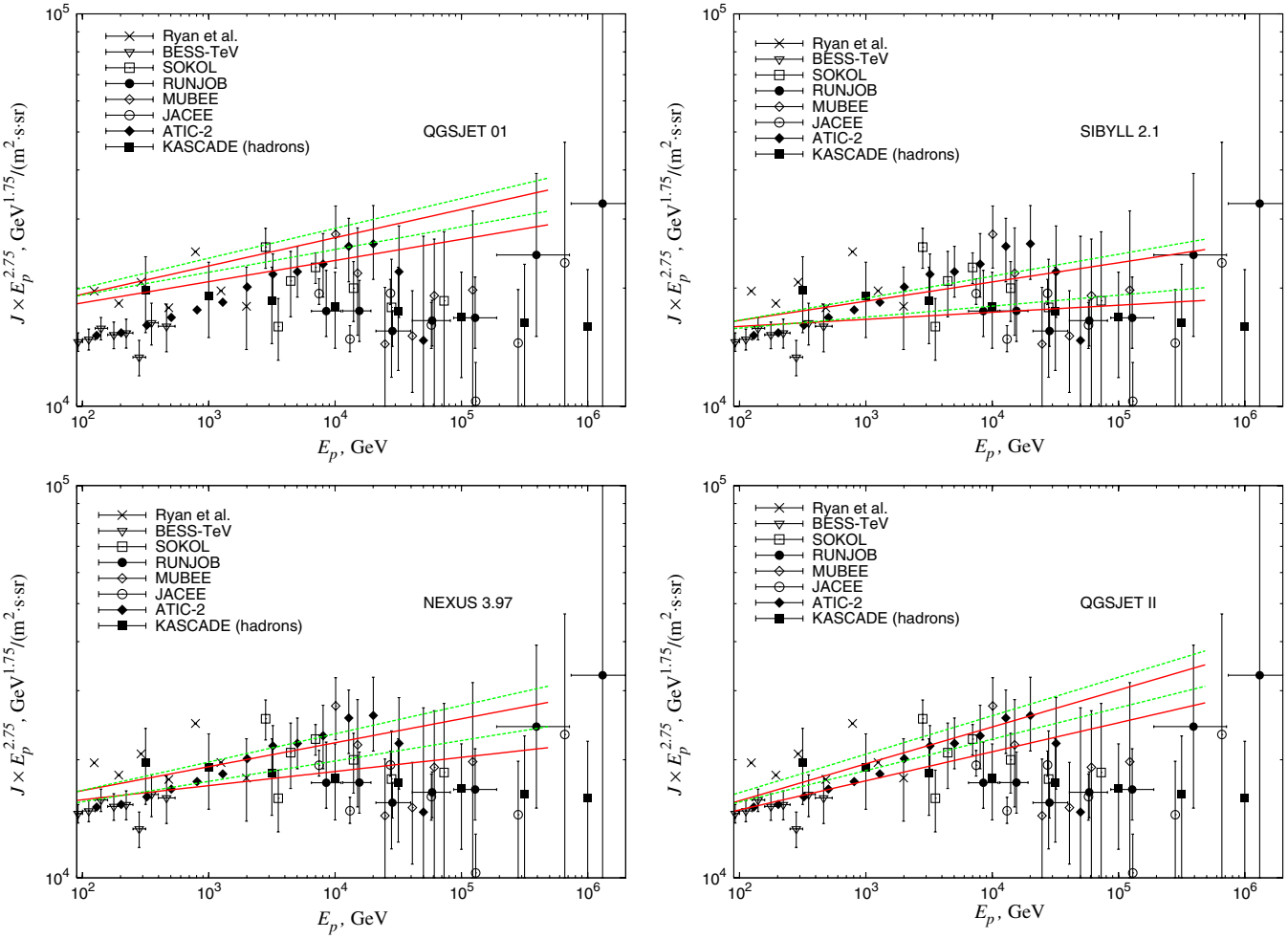

FIG. 5 (color online). Primary proton spectrum. Experimental data: [50] Ryan *et al.*, [42] BESS-TeV, [51] SOKOL, [9] RUNJOB, [52] MUBEE, [10] JACEE, [53] ATIC-2, [38] KASCADE (hadrons). Solid lines and dashed lines show primary proton spectra for muon flux parametrizations (1) and (2) correspondingly. Upper and lower lines reflect uncertainty in helium flux according to [34].

TABLE I. Parameters of primary proton spectrum fits $J_p = AE^{-\gamma}$, $(\mathrm{cm}^2\,\mathrm{s}\,\mathrm{sr}\,\mathrm{GeV})^{-1}$, for muon spectrum parametrization (2).

Low helium flux							
	No break		With break				
Model			Below break		Break	Above break	
	A	γ	A	γ	(TeV)	A	γ
QGSJET 01	1.42	2.675	0.93	2.620	15	3.25	2.750
QGSJET II	1.04	2.650	0.69	2.595	10	2.39	2.730
NEXUS 3.97	1.22	2.680	1.01	2.655	13	1.78	2.715
SIBYLL 2.1	1.29	2.695					
High helium flux							
	No break		With break				
Model			Below break		Break	Above break	
	A	γ	A	γ	(TeV)	A	γ
QGSJET 01	1.45	2.690	0.95	2.635	15	3.65	2.775
QGSJET II	1.08	2.670	0.69	2.610	14	3.18	2.770
NEXUS 3.97	1.25	2.700	1.01	2.670	12	2.14	2.750
SIBYLL 2.1	1.37	2.720					

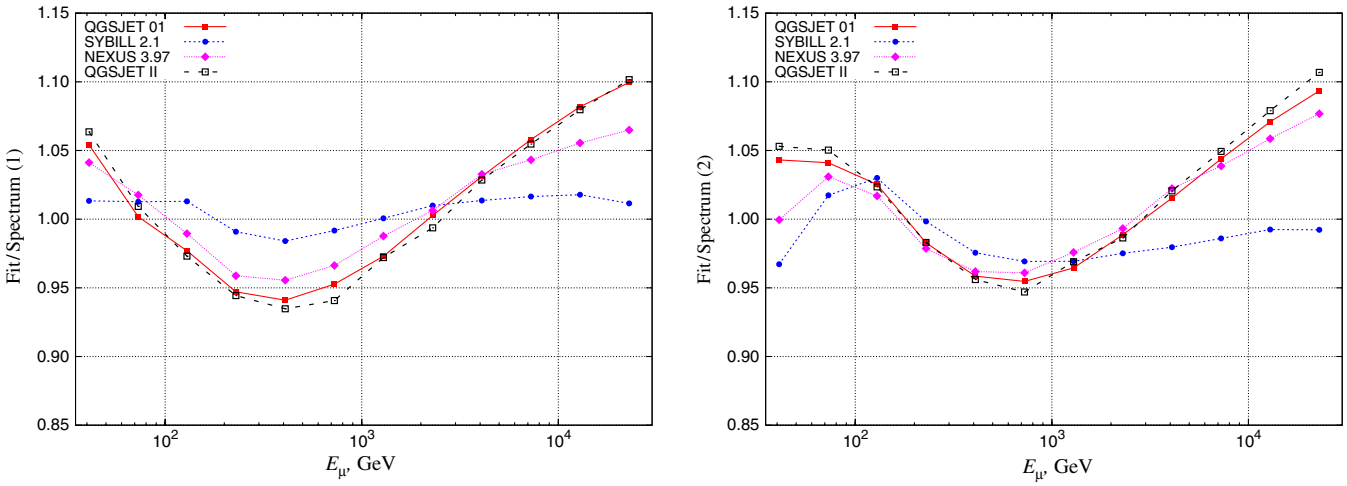

FIG. 6 (color online). Ratios of muon fluxes, obtained for power-law primary proton spectra, given in Fig. 5, to muon flux parametrizations (1) and (2).

II and NEXUS 3.97 models are in the best agreement with ATIC-2 data, while SIBYLL 2.1 provides intermediate between ATIC-2 and emulsion chambers experiments slope value. Spectra, reconstructed from parametrization

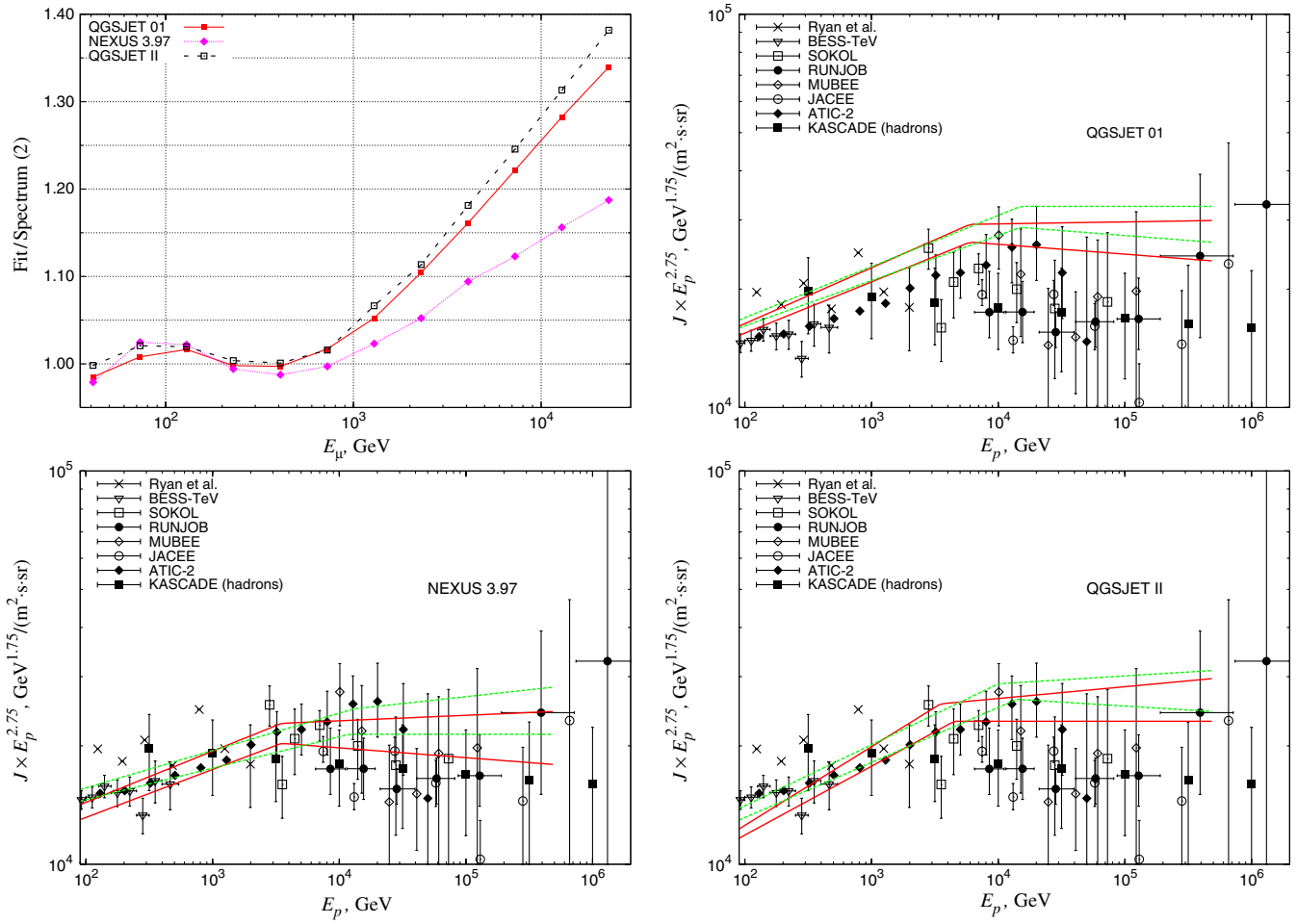

FIG. 7 (color online). Upper left panel shows ratios of muon fluxes, obtained for primary proton spectra with constant power indices equal to those before break, to muon flux parametrization (2). Other designations as in Fig. 5.

(1), have breaks at 3–6 TeV and in the case of QGSJET II proton flux poorly agrees with experiments at primary energies around 100 GeV. Evidently, the latter problems are explained by too low, in comparison with underground data, muon flux and this parametrization is considered here mostly for estimation of sensitivity of primary spectrum features to the choice of reference muon flux.

It is necessary to note that, due to low sensitivity of differential muon flux to helium and heavier groups of primary nuclei, it is impossible to derive any conclusions on the presence of the break in these PCR components. For illustration let us consider the example of calculations for QGSJET 01 and high helium flux, where the break in proton spectrum is positioned at $E_{\rm br} = 15$ TeV and the change of power index is equal to 0.14 (see Table I). Introduction of the rigidity-dependent break in He spectrum at $2E_{\rm br}$ per nucleus of the same value $\Delta\gamma = 0.14$ gives remarkable discrepancy between calculated muon spectrum and parametrization (2) only for energies above 7 TeV, which reaches 10% at 20 TeV. To correct this asymptotic behavior, it suffices to reduce $\Delta\gamma$ to 0.11 simultaneously for protons and helium without a change of the break position, and thus we get proton spectrum lying well within the corridor between parametrizations for high and low helium fits, shown in Fig. 7. Hence, this corridor covers all possible cases of He flux behavior (with or without break), provided the helium flux stays within limits, given in [34].

Summarizing we can say that primary proton spectrum shape turns out to be sensitive to the choice of interaction model and allows the presence of break at 10–15 TeV with $\Delta\gamma_p$ up to 0.15, which can be slightly softened though, if to allow the presence of the same break in other PCR components spectra.

VI. HADRONS

A comparison of our calculations of hadron spectrum for the primary spectra from [34] (high helium flux) with the recent measurements, performed by EAS-TOP collaboration [12], is presented in Fig. 8 (left panel). First, let us note the following facts. Below 100 GeV all calculated spectra have breaks, caused by nonperfect matching of low-energy interaction model GHEISHA to the high-energy models. Shape of the measured hadron spectra also breaks at energies above 4 TeV and the data become less definite, thus in the forthcoming analysis we are going to consider the data for energies from 129 GeV to 4 TeV. For these energies QGSJET 01, QGSJET II, and SIBYLL 2.1 quite reasonably reproduce the shape of the measured hadron spectrum, NEXUS 3.97 leads to spectrum with almost constant power index. One can see that the most consistent description of the data for specified energies provide QGSJET 01 and SIBYLL 2.1. In contrast with the muons there are no energy range, where the models agree on the hadron fluxes and the reasons of this disagreement are not as simple to point out as in the case with muons. The most important characteristics in this analysis are total inelastic cross section, determining chances of primary particle to survive, shapes of inclusive spectra $p + A \rightarrow p + X$, $p + A \rightarrow n + X$, $\pi^{\pm} + A \rightarrow \pi^{\pm} + X$ in the very forward region, responsible for substantial process of leading particles production (see Fig. 9 for the listed spectra). Let us briefly outline the major conclusions, which one may come to in the given situation. NEXUS 3.97 gives the lowest fluxes as of hadrons in total, so of nucleons and mesons (Fig. 10), and this happens in spite of the lowest inelastic cross-section values. Inclusive spectrum $p + A \rightarrow p + X$ immediately helps to figure out that incident protons in NEXUS 3.97 have comparably low chances to save most of their energy in collision and this leads to such low nucleon flux; the same can be said about meson flux and production of pions by pions. Similarly, from comparison of the inclusive spectra, it can be easily understood why QGSJET II gives the highest hadron flux. Note that SIBYLL 2.1 concedes to QGSJET II in hadron intensity mostly because of less effective production of leading neutrons in p-air collisions and due to the larger total interaction cross section.

Thus, from analysis of the data on hadron flux it is difficult to imply any strict constraints on inclusive spectra shapes, since the mechanism of hadron spectrum formation is more sophisticated than that in the case of muon spectrum. SIBYLL 2.1 and QGSJET 01 display quite different behaviors of the relevant inclusive spectra and total interaction cross sections, but both models almost equally succeed in description of the EAS-TOP data (i.e. produce close hadron fluxes).

The given standard approach to analysis of situation, in fact, is of little sense, since it is based on assumption about validity of primary spectra in the form of fits from [34], which was called into question in our previous discussion. In this case it is logical to analyze interaction models self-consistency, i.e. their ability to give correct estimates of several CR components at once. Provided we know the behavior of primary proton spectra for every model, required to match the data on muon flux, we may check how these proton spectra agree with the data on hadrons. In Fig. 8 (right panel) we give hadron intensities, calculated for primary proton spectra with breaks from Fig. 7 (for SIBYLL 2.1 see Fig. 5), corresponding to muon spectrum parametrization (2). After an increase of primary nucleon flux, dictated by the data on muons, one can see that the best agreement with EAS-TOP measurement provide NEXUS 3.97 and SIBYLL 2.1. It would be interesting to note that two models with different philosophies and inclusive spectra give the most self-consistent results on muons and hadrons, but, of course, this conclusion must be taken with much care, since it is based on the single set of data and we have only indirect indications on the accuracy of this set, e.g. such as agreement of primary

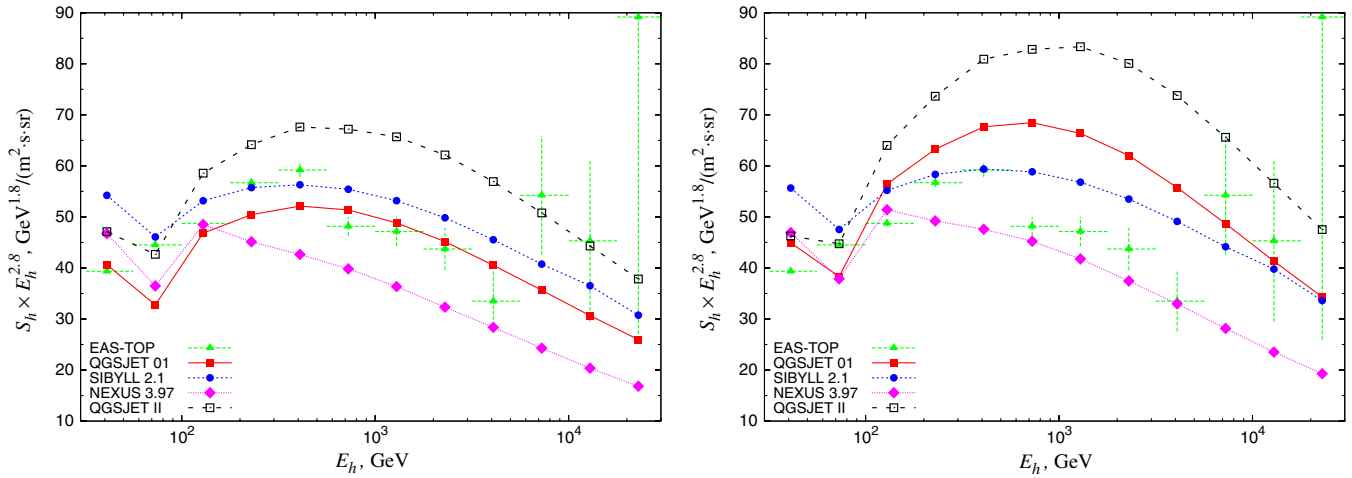

FIG. 8 (color online). Hadron spectra at the EAS-TOP depth $t = 820$ g/cm^2. Left: Calculations for primary spectra from [34] with high helium flux. Right: Calculations for proton spectra from Fig. 7 (for SIBYLL 2.1 from Fig. 5).

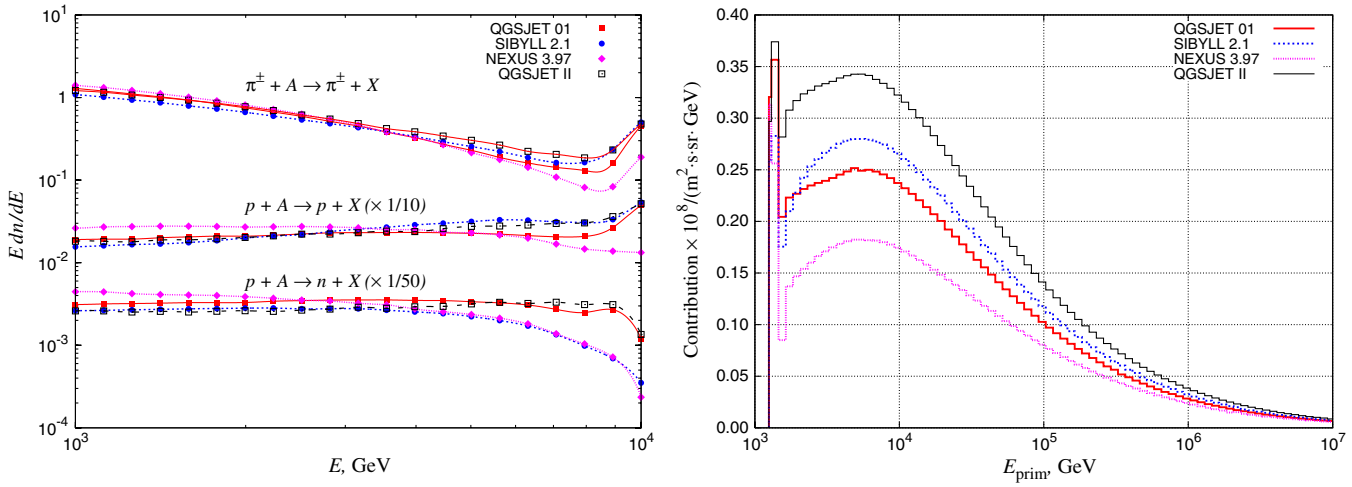

FIG. 9 (color online). Left: Inclusive spectra $\pi^{\pm} + A \to \pi^{\pm} + X$, $p + A \to p + X$ (scaled down by 10), $p + A \to n + X$ (scaled down by 50) for incident particles with energy 10 TeV. Right: Contribution of primary particles with energies $E_{\rm prim}$ to the hadron differential spectrum $S_{\rm h}(E_{\rm h})$ at 820 g/cm^2 for $E_{\rm h} = 1.29$ TeV .

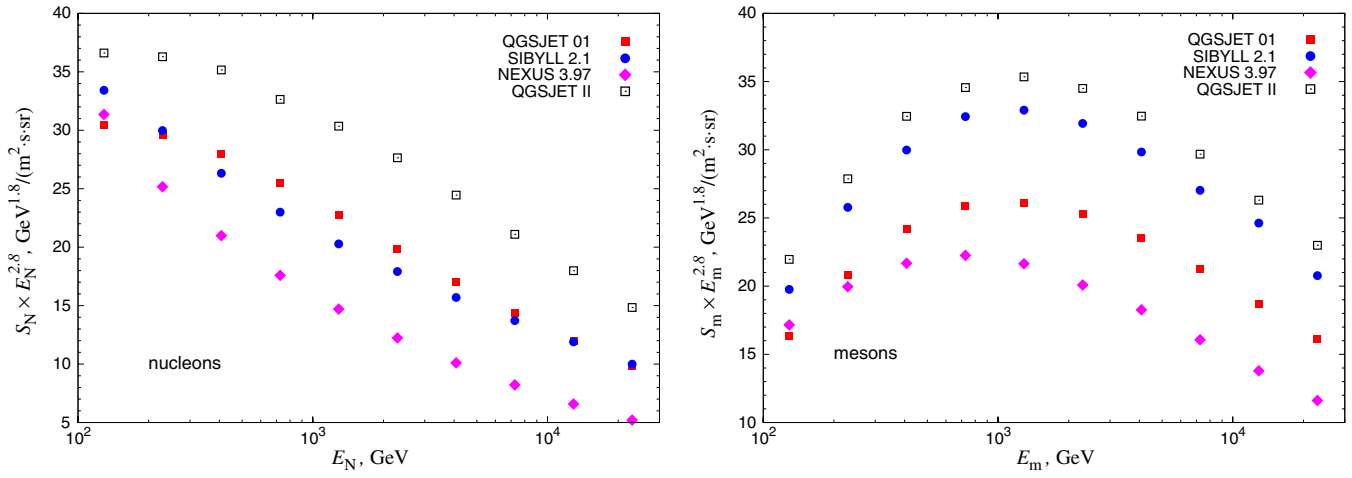

FIG. 10 (color online). Spectra of nucleons (left) and mesons (right) at 820 g/cm^2 for primary spectra [34] with high helium flux.

proton fluxes, obtained by EAS-TOP and KASCADE teams (the latter is derived from flux of unaccompanied hadrons [38]). If we try to perform the same analysis with the variety of the data, obtained at different atmospheric altitudes and zenith angles, no consistent notions of such kind will be obtained as can be easily seen from calculations, presented in [11].

VII. CONCLUSIONS

The progress in CR and high-energy physics achieved during the past 10–15 years allowed one to turn from statements about satisfactory (qualitative) concordance between different kinds of data to investigation of more fine effects. As an example, we managed to show that reconstructed from the data on vertical muon flux primary proton spectra have not only expected interaction model-dependent intensities, but also model-dependent shapes. It is demonstrated that application of QGSJET 01, QGSJET II, and NEXUS 3.97 models brings to proton spectrum with a break at 10–15 TeV and power index γ_p before a break close to that, measured in the ATIC-2 experiment. Nevertheless one can see that absolute proton flux for QGSJET 01 is hardly compatible with any data of direct experiments, and the break for all these three models is more moderate, compared to what can be inferred from ATIC-2 data, which though become less definite right in the break region. On the other hand, SIBYLL 2.1 allows one to reproduce shape of the muon spectrum with single power-law proton spectrum, which is in reasonable agreement with both emulsion chamber and ATIC-2 data within experimental errors. Further improvement of our understanding of the situation, which is of primary astrophysical interest, can be achieved via experimental study as of muon CR component characteristics with water and ice neutrino telescopes and so of inclusive spectra $p + A \rightarrow \pi^{\pm}, K^{\pm}$ in the fragmentation region. Reduction of uncertainties in the latter component with the use of the data on primary spectra, hadron, and muon components does not look possible because of (1) poor correlation between muon and hadron production mechanisms, (2) ambiguity of existing CR experimental data, and (3) possibility to realize self-consistent description of the data on muons and hadrons with the models, having remarkably differing inclusive spectra and underlying philosophies.

ACKNOWLEDGMENTS

The authors greatly acknowledge the CONEX team and personally Tanguy Pierog for their kind permission to use CONEX cross-section tables and for technical support. We are grateful to an anonymous referee for constructive remarks, which helped us to improve the manuscript. This work was supported in part by RFBR Grant No. 07-02-01154-a.

[1] N. L. Grigorov, I. D. Rapoport, and V. Y. Shestoperov, *High Energy Particles in Cosmic Rays* (Nauka, Moscow, 1973).
[2] T. H. Burnett *et al.*, Nucl. Instrum. Methods Phys. Res., Sect. A **251**, 583 (1986).
[3] I. V. Rakobolskaya, V. V. Kopenkin, and A. K. Managadze, *Interaction Characteristics of Ultra High Energy Cosmic Ray Hadrons* (Moscow State University, Moscow, 2000).
[4] A. V. Apanasenko *et al.*, Astropart. Phys. **16**, 13 (2001).
[5] A. A. Lagutin, A. G. Tyumentsev, and A. V. Yushkov, J. Phys. G **30**, 573 (2004).
[6] A. A. Lagutin, A. G. Tyumentsev, and A. V. Yushkov, Phys. At. Nucl. **69**, 272 (2006).
[7] A. D. Panov *et al.*, Bull. Russ. Acad. Sci. Phys. **71**, 494 (2007).
[8] V. I. Zatsepin and N. V. Sokolskaya, Astron. Astrophys. **458**, 1 (2006).
[9] V. A. Derbina *et al.* (RUNJOB Collaboration), Astrophys. J. **628**, L41 (2005).
[10] K. Asakimory *et al.*, Astrophys. J. **502**, 278 (1998).
[11] A. A. Kochanov, T. S. Sinegovskaya, and S. I. Sinegovsky, arXiv:astro-ph/0803.2943.
[12] M. Aglietta *et al.* (EAS-TOP Collaboration), Astropart. Phys. **19**, 329 (2003).
[13] R. S. Fletcher, T. K. Gaisser, P. Lipari, and T. Stanev, Phys. Rev. D **50**, 5710 (1994).
[14] R. Engel, T. K. Gaisser, P. Lipari, and T. Stanev, in *Proceedings of the 26th International Cosmic Ray Conference* (The University of Utah, Salt Lake City, UT, 1999), Vol. 1, pp. 415–418.
[15] H. J. Drescher *et al.*, Phys. Rep. **350**, 93 (2001).
[16] A. A. Lagutin, Altai State University Report No. ASU 94/1, 1994.
[17] A. A. Lagutin and A. V. Yushkov, Phys. At. Nucl. **69**, 460 (2006).
[18] I. A. Sokalski, E. V. Bugaev, and S. I. Klimushin, Phys. Rev. D **64**, 074015 (2001).
[19] P. Antonioli *et al.*, Astropart. Phys. **7**, 357 (1997).
[20] L. N. Bogdanova, M. G. Gavrilov, V. N. Kornoukhov, and A. S. Starostin, Phys. At. Nucl. **69**, 1293 (2006).
[21] M. Aglietta *et al.*, Phys. Rev. D **58**, 092005 (1998).
[22] Y. M. Andreyev, V. I. Gurentsov, and I. M. Kogai, in *Proceedings of the 20th International Cosmic Ray Conference* (Nauka, Moscow, USSR, 1987), Vol. 6, pp. 200–203.
[23] W. Rhode, Nucl. Phys. B, Proc. Suppl. **35**, 250 (1994).
[24] C. Berger *et al.* (Frejus Collaboration), Z. Phys. C **48**, 221 (1990).
[25] M. Ambrosio *et al.*, Phys. Rev. D **52**, 3793 (1995).
[26] K. Ruddick, Report No. PDK-435, 1990.

[27] S. M. Kasahara, Ph.D. thesis, University of Minnesota, 1997.
[28] T. Pierog *et al.*, Nucl. Phys. B, Proc. Suppl. **151**, 159 (2006).
[29] T. Bergmann *et al.*, Astropart. Phys. **26**, 420 (2007).
[30] N. N. Kalmykov, S. S. Ostapchenko, and A. I. Pavlov, Nucl. Phys. B, Proc. Suppl. **52**, 17 (1997).
[31] S. Ostapchenko, Nucl. Phys. B, Proc. Suppl. **151**, 143 (2006).
[32] S. Ostapchenko, Phys. Rev. D **74**, 014026 (2006).
[33] S. Ostapchenko, Phys. Lett. B **636**, 40 (2006).
[34] T. K. Gaisser and M. Honda, Annu. Rev. Nucl. Part. Sci. **52**, 153 (2002).
[35] E. V. Bugaev *et al.*, Phys. Rev. D **58**, 054001 (1998).
[36] A. A. Lagutin, A. G. Tyumentsev, and A. V. Yushkov, Int. J. Mod. Phys. A **20**, 6834 (2005).
[37] A. A. Lagutin, A. G. Tyumentsev, and A. V. Yushkov, Nucl. Phys. B, Proc. Suppl. **175–176**, 555 (2008).
[38] T. Antoni *et al.* (KASCADE Collaboration), Astrophys. J. **612**, 914 (2004).
[39] M. Aglietta *et al.* (LVD Collaboration), Phys. Rev. D **60**, 112001 (1999).
[40] V. A. Kudryavtsev, N. J. C. Spooner, and J. E. McMillan, Nucl. Instrum. Methods Phys. Res., Sect. A **505**, 688 (2003).
[41] P. Achard *et al.* (L3 Collaboration), Phys. Lett. B **598**, 15 (2004).
[42] S. Haino *et al.*, Phys. Lett. B **594**, 35 (2004).
[43] B. C. Rastin, J. Phys. G **10**, 1609 (1984).
[44] V. N. Bakatanov *et al.*, Sov. J. Nucl. Phys. **55**, 1169 (1992).
[45] R. I. Enikeev *et al.*, Sov. J. Nucl. Phys. **47**, 665 (1988).
[46] G. T. Zatsepin *et al.*, Bull. Russ. Acad. Sci. Phys. **58**, 2050 (1994).
[47] M. Crouch, in Proceedings of the 20th International Cosmic Ray Conference, Ref. [22], pp. 165–168.
[48] M. Robinson *et al.*, Nucl. Instrum. Methods Phys. Res., Sect. A **511**, 347 (2003).
[49] M. Aglietta *et al.* (LVD Collaboration), Astropart. Phys. **3**, 311 (1995).
[50] M. J. Ryan, J. F. Ormes, and V. K. Balasubrahmanyan, Phys. Rev. Lett. **28**, 985 (1972).
[51] I. P. Ivanenko *et al.*, in *Proceedings of the 23rd International Cosmic Ray Conference* (The University of Calgary, Calgary, Canada, 1993), Vol. 2, pp. 17–20.
[52] V. I. Zatsepin *et al.*, in Proceedings of the 23rd International Cosmic Ray Conference, Ref. [51], pp. 13–16.
[53] J. P. Wefel *et al.*, in *Proceedings of the 29th International Cosmic Ray Conference* (Tata Institute of Fundamental Research, Pune, India, 2005), Vol. 3, pp. 105–108.